Circular-dichroism enantiomers assisted Full-Poincaré Polarization wavefront manipulation metasurface: supplement

YANG CHENG, YONGFENG LI,* HE WANG, JIAFU WANG, WEIPENG WAN, QI YUAN, LIN ZHENG, JIEQIU ZHANG, AND SHAOBO QU

Department of Basic Sciences, Air Force Engineering University, Xi'an, Shanxi 710051, China
liyf217130@126.com

Supporting Information

Circular-dichroism enantiomers assisted Full-Poincaré Polarization wavefront manipulation metasurface

Yang Cheng, Yongfeng Li*, He Wang, Jiafu Wang, Weipeng Wan, Qi Yuan, Lin Zheng, Jieqiu Zhang, and Shaobo Qu
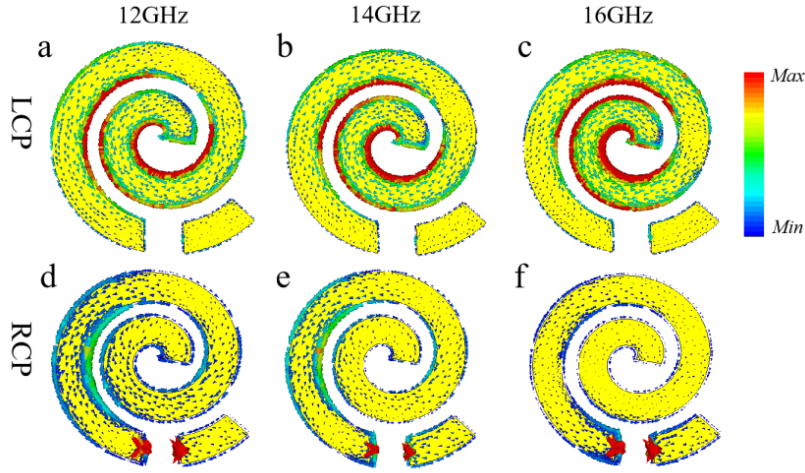
S1. The surface current analysis

Fig S1. The simulation results of surface current on Archimedean spiral structure. a, b, and c) surface current distribution of R-enantiomer at incident LCP plane wave at 12GHz, 14GHz, and 16GHz respectively. d, e, and f) surface current distribution of R-enantiomer at incident RCP plane wave at 12GHz, 14GHz, and 16GHz respectively.

S2. The FPP customized table

Table S1. The left column is the spin orientation and AR, and the uppermost column is the polarization azimuth. The corresponding rotation angles of each atom are shown in the table below, where $rot_1=0°$.

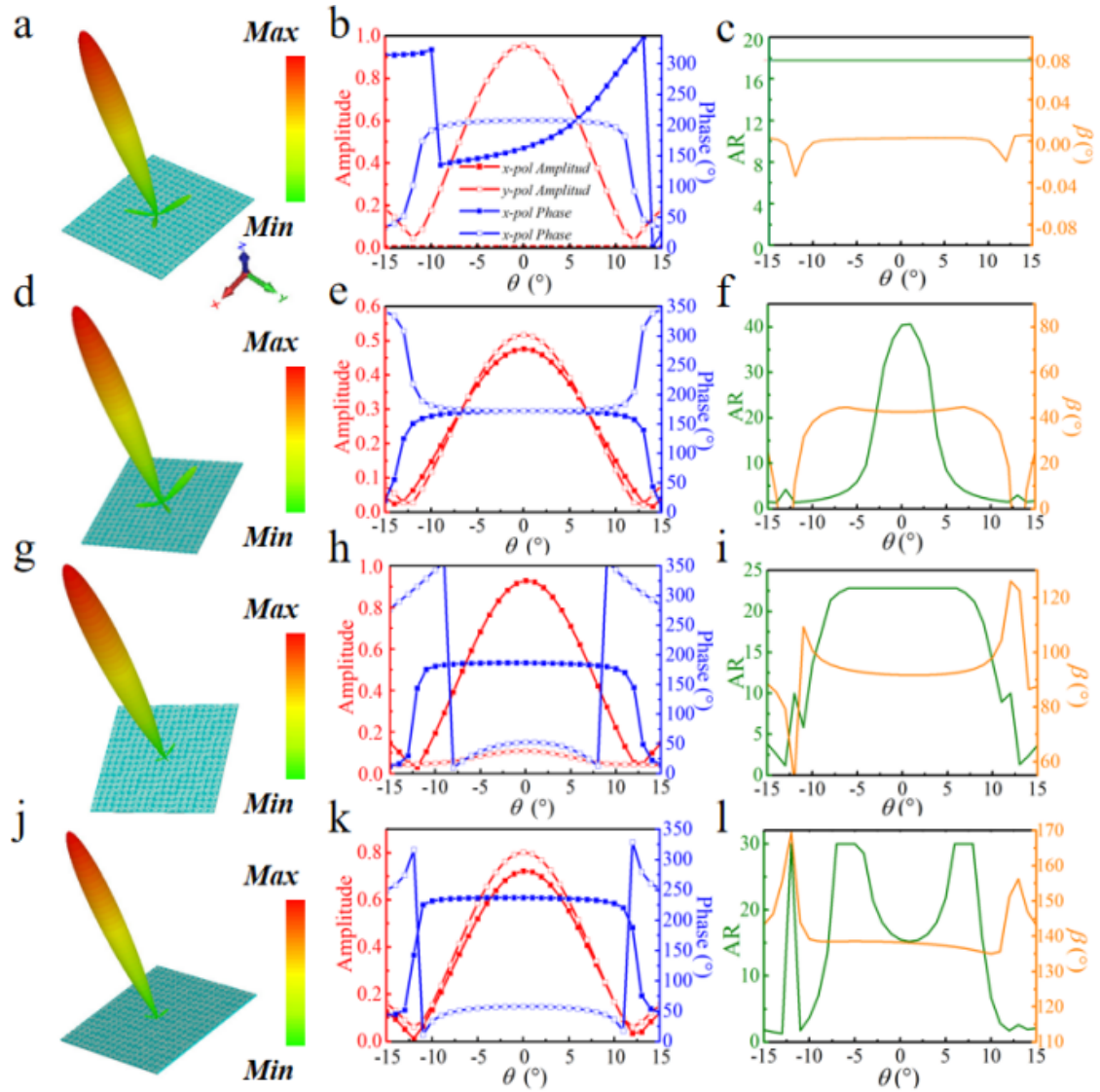| Azimuth / State	0°	45°	90°	135°
0 (LP)	$rot_2=0°$, $rot_3=0°$, $rot_4=0°$	$rot_2=45°$, $rot_3=0°$, $rot_4=0°$	$rot_2=90°$, $rot_3=0°$, $rot_4=0°$	$rot_2=135°$, $rot_3=0°$, $rot_4=0°$
1/3 (ELCP)	$rot_2=-30°$, $rot_3=0°$, $rot_4=30°$	$rot_2=15°$, $rot_3=0°$, $rot_4=75°$	$rot_2=60°$, $rot_3=0°$, $rot_4=120°$	$rot_2=105°$, $rot_3=0°$, $rot_4=165°$
1(LCP)	$rot\,2=0°$, $rot\,3=0°$, $rot\,4=90°$			
-1(RCP)	$rot\,2=0°$, $rot\,3=90°$, $rot\,4=0°$			

S3. Simulation results of L-pol manipulation with different *β*.

Figure S2. a, d, g, and j) Three-dimensional far-field scattering pattern of normal L-pol manipulation with *β* = 0°, 45°, 90°, and 135°. b, e, h, and k) Simulation results of phase and amplitude of *x*- and *y*-pol at *φ*=0°, corresponding to normal L-pol modulation with *β* = 0°, 45°, 90°, and 135°, respectively. c, f, i, and l) Calculated results of AR and polarization azimuth at *φ*=0°, corresponding to normal L-pol modulation with *β* = 0°, 45°, 90°, and 135°, respectively.

S4. The simulation results of 3-AR left-spin-elliptic polarization manipulation with different *β*.
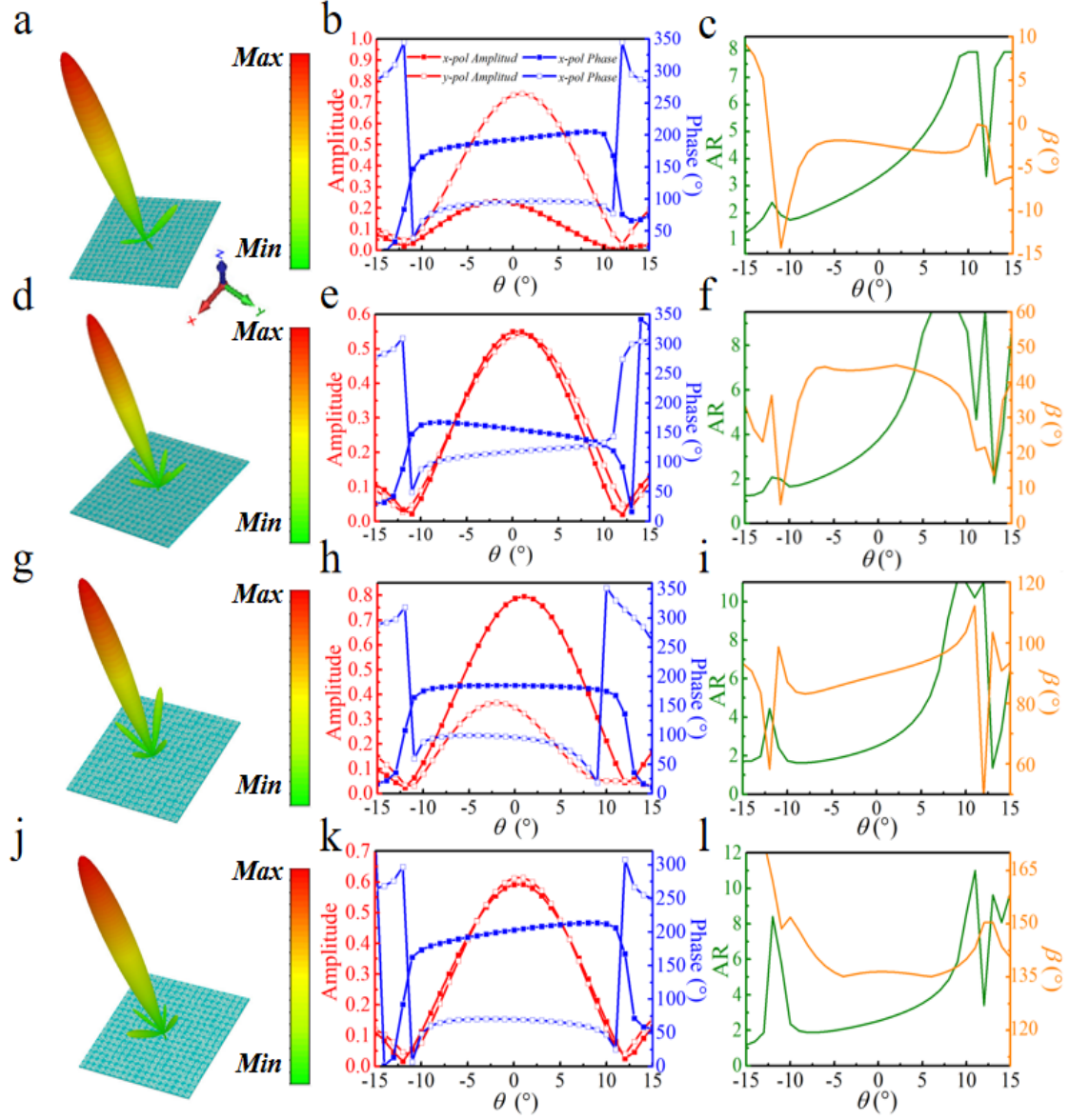

Figure S3. a, d, g, and j) Three-dimensional far-field scattering pattern of normal 3-AR left-spin-elliptic polarization manipulation with *β* = 0°, 45°, 90°, and 135°. b, e, h, and k) Simulation results of phase and amplitude of *x*- and *y*-pol at *φ*=0°, corresponding to normal 3-AR left-spin-elliptic polarization modulation with *β* = 0°, 45°, 90°, and 135°, respectively. c, f, i, and l) Calculated results of AR and polarization azimuth at *φ*=0°, corresponding to normal 3-AR left-spin-elliptic polarization modulation with *β* = 0°, 45°, 90°, and 135°, respectively.

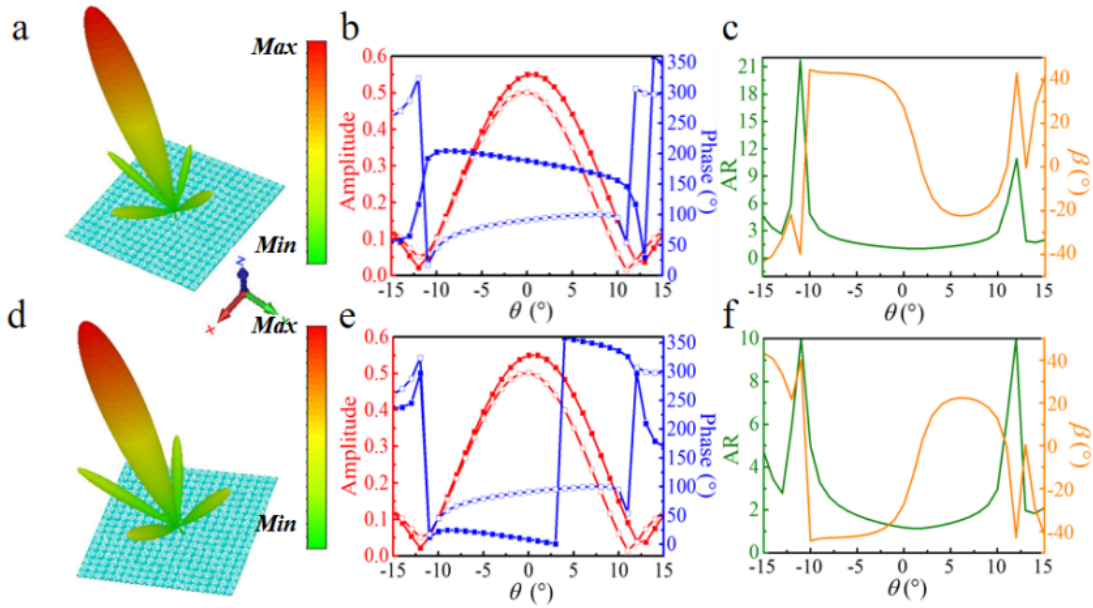## S5. Simulation results of LCP and RCP manipulation.

Figure S4. a, c) Three-dimensional far-field scattering pattern of normal polarization manipulation of RCP and LCP. b, d) Simulation results of phase and amplitude of x- and y-pol at $\varphi=0°$, corresponding to normal polarization modulation of RCP and LCP, respectively.

S6. Combination of GA and L-BFGS-B

GA is suitable for solving some discrete numerical and non-numerical problems. At the same time, it has excellent global optimization ability. The disadvantage is that the optimization efficiency significantly reduces when approaching the optimal value, and the optimal value is not even obtained. L-BFGS-B, a quasi-Newton method, is suitable for solving some nonlinear equations and has faster local convergence, but it has higher initial value requirements. As for why to use genetic algorithms to calculate a global approximate optimal solution first, it is because the introduction of CD enantiomers leads to the discretization of the optimization problem. Simultaneously, GA could provide a globally better initial value for gradient-based optimization algorithms. Here, the chirality v of each element is determined by GA, and the phase profile optimized by GA is set as the initial values of the gradient-based optimization algorithms to solve the Local optimization problem.

S7. Simulated results of polarization and normalized energy in K-space of GA-based bi-atom metasurface.
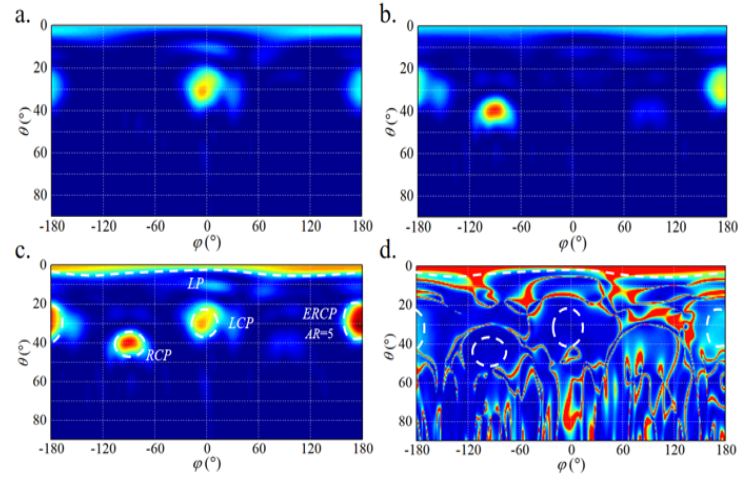
Figure S5. a, b, and c) K-space normalized amplitude distribution of the RCP, the LCP, and the synthetic polarization. d) Axial ratio distribution of synthetic polarization in K-space.